VARIABILITY AND CHANGES OF DAILY CLIMATE EXTREMES OVER THE CORE CROP REGION OF ARGENTINA

Miguel A. LOVINO[1], Omar V. MÜLLER[1], Ernesto H. BERBERY[2], Gabriela V. MÜLLER[1], Maria del Valle VENENCIO[1], Leandro C. SGROI[1], Maria Agostina BRACALENTI[1]

[1]*Centro de Variabilidad y Cambio Climático (CEVARCAM), Facultad de Ingeniería y Ciencias Hídricas, Universidad Nacional del Litoral, Santa Fe, Argentina.*

[2]*Earth System Science Interdisciplinary Center/Cooperative Institute for Climate and Satellites-Maryland, University of Maryland, College Park, United States.*

mlovino@unl.edu.ar, gvmuller@fich.unl.edu.ar, **mvallevenencio@gmail.com**

ABSTRACT

Variability and changes in climate extremes affect the core crop region of Argentina and may increase its vulnerability leading to unprecedented disasters. This study investigates the long-term changes and interannual variability of daily temperature and precipitation climate extremes and assesses to what extent global reanalyses reproduce the observed variability in the recent past. Datasets include quality-controlled observations (1963-2013) and ERA-Interim and NCEP2 reanalyses (1979-2011). Climate extremes are characterized spatially and temporally by 11 indices proposed by the Expert Team on Climate Change Detection and Indices. A Singular Spectrum Analysis was applied to detect the leading modes of the area-averaged index time series. Nonparametric linear trends were fitted to each index time series to estimate the spatial distribution of mean changes. Temperature extremes are changing towards warmer conditions. Warm days has been increasing since 1990 while cold days has been decreasing. Warm and cold nights show a significant signal of warming that seems to be stabilizing in recent decades. Intense precipitation events in most of the region increased steadily since 1970. The annual maximum amount of 1-day precipitation events increased from the 1970s to the 2000s, stabilizing in recent years. The ERA-Interim reanalysis can recognize temperature extremes in time and space, while the older NCEP2 presents systematic biases. Both reanalyses reproduce the annual maximum 5-day precipitation with large biases. Although reanalyses would be expected to add information for climate extremes in areas of scarce observations, they still need to be used with great caution and only as a complement to observations.

Key words: climate extremes, intense precipitation, warm/cold days/nights, ERA-Interim reanalysis, NCEP2 reanalysis.

RESUMEN

La variabilidad y los cambios en extremos climáticos afectan la región núcleo de cultivos de Argentina y pueden incrementar su vulnerabilidad ocasionando desastres sin precedentes. Este estudio investiga los cambios de largo período y la variabilidad

interanual de los extremos climáticos diarios de precipitación y temperatura y evalúa en qué medida los reanálisis globales reproducen la variabilidad observada en el pasado reciente. Los datos incluyen observaciones con calidad controlada (1963-2013) y los reanálisis ERA-Interim y NCEP2 (1979-2011). Los extremos climáticos se caracterizan espacial y temporalmente con 11 índices de los propuestos por el Equipo de Expertos sobre Detección e Índices de Cambio Climático. Se aplicó un Análisis Espectral Singular para detectar los modos principales de las series temporales medias areales de los índices. Se ajustaron tendencias no-paramétricas lineales a las series temporales de cada índice para estimar la distribución espacial de los cambios medios. Los extremos de temperatura están cambiando hacia condiciones más cálidas. Los días cálidos han estado aumentando desde 1990 mientras que los días fríos han ido decreciendo. Las noches cálidas y frías muestran una señal de calentamiento significativa que parece estar estabilizándose en las últimas décadas. Los eventos de precipitación intensa aumentaron constantemente en la mayor parte de la región desde 1970. La cantidad máxima anual de precipitación en un día aumentó desde la década de 1970 hasta la del 2000, estabilizándose en años recientes. El reanálisis ERA-Interim puede reconocer los extremos de temperatura en tiempo y en espacio, mientras que el antiguo NCEP2 presenta errores sistemáticos. Ambos reanálisis reproducen la máxima precipitación anual en 5 días con grandes sesgos. Aunque se esperaría que los reanálisis agreguen información para extremos climáticos en áreas de observaciones escasas, aún deben usarse con mucha precaución y solo como complemento de las observaciones.

Palabras clave: extremos climáticos, precipitación intensa, días cálidos/fríos, noches cálidas/frías, reanálisis ERA-Interim, reanálisis NCEP2.

1. INTRODUCTION

Extreme weather and climate events affect ecosystems, disrupt food production, and impact negatively human settlements causing morbidity and mortality (Magrin et al., 2014). In South America during the last decade (2007-2016), extreme weather and climate events have led to about 7,000 fatalities, more than 58 million people affected, and estimated losses of US$ 24 billion (Guha-Sapir et al., 2015). Frequent and intense precipitation extremes have favored recurrent floods in urban and rural areas (Magrin et al., 2014). Extreme climate events in this continent have increased in the last decades as reflected in changes in daily extremes of precipitation and temperature (e.g., Skansi et al., 2013 and references therein). Towards southeastern South America a moderate confidence of a warming in temperature extremes and an increase of intense precipitation events has been detected (e.g., Cavalcanti et al., 2015; Carril et al., 2016 and references therein). Also consistent with global trends, the number of cold nights has decreased and warm nights has increased, the number of warm days has increased and cold days have become fewer (Rusticucci et al., 2016).

This research focuses on the core crop region that covers the fertile soils of the Pampas and Chaco plains in Northeastern Argentina (NEA; see Fig. 1a). This region has great economic and demographic significance as it concentrates most of the

agricultural production and the population of the country. This study investigates the long-term changes and interannual variability of daily temperature and precipitation extremes, and assesses to what extent ERA-Interim and NCEP2 reanalyses reproduce the observed variability in the recent past over the core crop region in Argentina.

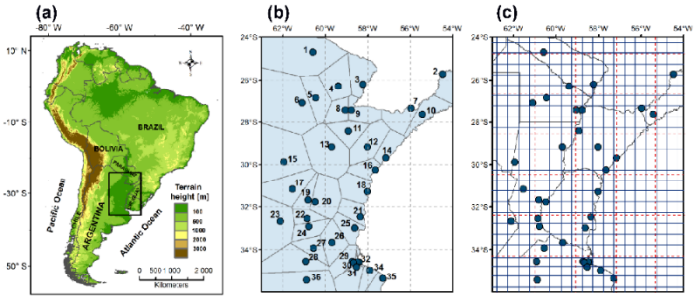

Fig. 1: (a) South America and the study region in northeastern Argentina (black rectangle). (b) Stations with in-situ observations and the Thiessen polygons used to compute the areal-average of the variables. (c) Reanalyses grid resolution: ERA-Interim (blue full lines) and NCEP2 (red dashed lines). Source: Lovino et al. (2018)

2. METHODOLOGY

In-situ observations of daily precipitation as well as daily maximum and minimum temperatures for 1963-2013 were used. About 36 stations were selected for the quality and extent of the records (see Fig. 1b). To be included, stations were required to exceed a threshold of 90% of days with data availability. Missing values were filled using the normal ratio method to interpolate from nearby stations (Young et al., 1992). A quality control of the completed time series was carried out to identify non-systematic errors, ensure the absence of outliers and the internal consistency of the records. The ERA-Interim (Dee et al., 2011) and the NCEP-DOE Reanalysis 2 (NCEP2, Kanamitsu et al., 2002) were used for the common period from 1979 to 2011. The ERA-Interim is used on a regular grid at 0.5° spatial resolution, while the NCEP2 spatial resolution is 1.875° latitude x 1.904° longitude (see Fig. 1c).

We employ a subset of indices proposed by the Expert Team on Climate Change Detection and Indices (ETCCDI) that characterize the frequency, intensity and duration of climate extreme events (Klein Tank et al., 2009; see Table 1). The indices were evaluated in space and time. The 1981-2010 period was selected as the base period for the calculation of percentile indices and to compute anomalies of the other indices. Area-averaged time series were computed using the Thiessen Polygons method in each time step to take into account the uneven spatial distribution of the stations (see Fig. 1b).

A Singular Spectrum Analysis (Ghil et al., 2001) was employed to obtain the nonlinear trends and the oscillatory leading modes of the area-averaged time series of each index. We use a window length M = 10 years; thus, interannual variability

represents the spectrum between 2 and 10 years. A 10-yr moving average was used in cases when the SSA method does not clearly detect nonlinear trends, i.e. when the errors of the eigenvalues overlap preventing the separation of a trend signal.
Changes in extreme climate events at each station were assessed by fitting linear trends to the indices in the 51-year period. The magnitudes of the trends were computed adapting the nonparametric Kendall's tau based slope estimator (Sen, 1968) and using the method proposed by Wang and Swail (2001). Trends of all indices were tested for statistical significance at the 95% confidence level.

Temperature-based Indices				
	Index	**Index Name**	**Index definition**	**Unit**
Frequency	TX90p	Warm days	Percentage of annual days when $TX_{ij} > TX_{in}90$	% days
	TX10p	Cold days	Percentage of annual days when $TX_{ij} < TX_{in}10$	% days
	TN90p	Warm nights	Percentage of annual days when $TN_{ij} > TN_{in}90$	% days
	TN10p	Cold nights	Percentage of annual days when $TN_{ij} < TN_{in}10$	% days
	SU25	Summer days	Annual number of days when $TX_{ij} > 25$ °C	days
	FD	Frost days	Annual number of days when $TN_{ij} < 0$ °C	days
Precipitation-based Indices				
Intensity	RX1day	Max 1-day precipitation	Annual maximum 1-day precipitation amount	mm
	RX5day	Max 5-day precipitation	Annual maximum consecutive 5-day precipitation amount	mm
	SDII	Simple daily intensity index	Annual total precipitation divided by the number of wet days (when pr ≥ 1 mm)	mm/day
Duration	CWD	Consecutive wet days	Maximum annual number of consecutive wet days (when pr ≥ 1 mm)	days
	CDD	Consecutive dry days	Maximum annual number of consecutive dry days (when pr < 1 mm)	days

Table 1: ETCCDI indices used in this study. TX_{ij} and TN_{ij} are the daily maximum and minimum temperature respectively on day i in period j. $TX_{in}90$ or $TX_{in}10$ ($TN_{in}90$ or $TN_{in}10$) are the calendar day 90^{th} or 10^{th} percentile of daily maximum (minimum) temperature calculated for a 5-day window centered on each calendar day n from the base period 1981-2010. Adapted from Lovino et al. (2018)

The skill of ERA-Interim and NCEP2 to reproduce climate extremes is assessed contrasting the spatial and temporal climatology fields against observations and using the Pearson correlation coefficient (r) by comparing data from each station with those from a reanalysis grid cell covering this station. The ability of the reanalyses to represent temperature extremes is evaluated by means of two fixed-threshold indices: summer days and frost days (SU25 and FD respectively; Table 1). These indices were selected because they avoid the complexity of percentile-based indices, which are difficult to replicate in reanalysis and because they are relevant to the agro-industrial activities in the region. For precipitation extremes, the annual maximum 5-day amount (RX5day, Table 1) is evaluated. It was chosen because reanalyses may have greater ability to reproduce the RX5day than the annual maximum 1-day amount (RX1day, Table 1). The reason is that 5-day precipitation events are usually of larger spatial scale than daily extreme precipitation events (Sillman et al., 2013).

3. RESULTS

3.1. Temperature-related climate extremes

Figures 2a-d present the indices characterizing the frequency of maximum-temperature extremes, including warm days (TX90p) and cold days (TX10p) (see Table 1). Fig. 2a reveals a nonlinear trend of the frequency of warm days, which had slightly decreased before the 1990s, but since then it has experienced a steady increase of about 5%. Despite the dispersion among the trends of TX90p for all stations (thin lines in Fig. 2a), they exhibit a common behavior. The spatial distribution of the trends in Fig. 2b reveals that most stations have increases of warm days, particularly towards the northeast. Only a few stations (7 out of 36) experienced a decrease, and it was non-significant. Warm days are also influenced by interannual variability with a periodicity close to 9 years which explains 30% of the variance of the total time series.

The area-averaged frequency of colds days presented in Fig. 2c reveals a decrease from 10% to 7.5% of days per year since about 1990 with an important interannual variability. The spatial distribution of the linear trends presented in Fig. 2d shows the largest decrease of cold days towards the east.

Figures 2e-h present the indices characterizing the frequency of minimum-temperature extremes, including warm nights (TN90p) and cold nights (TN10p) (see Table 1). Fig. 2e indicates that warm nights exhibit an area-averaged positive nonlinear trend, more evident from the late 1960s to the early 1980s. From 1980 to 2013, the trend is also positive but with lower magnitude. The individual stations trends (thin lines) exhibit smaller dispersion around the 1980s, with a marked dispersion increase during latter years. Aside from the trends, a 4-yr mode of variability explains almost 30% of the TN10p and TN90p variances. Fig. 2f shows that warm nights presents the greatest increases towards the north (1% to 2% of days per decade), with 11 out of 19 stations with significant rising trends. The mean trend of the frequency of cold nights (Fig. 2g), shows that there was about a 5% decrease in the frequency of cold nights from the 1960s to 1980s, that is, at the same time

when an increase of about 3% was observed in the frequency of warm nights (Fig. 2e). According to Fig. 2h, the decrease in cold nights occurred in the whole region, with 21 stations having significant trends at least at the 95% confidence level.

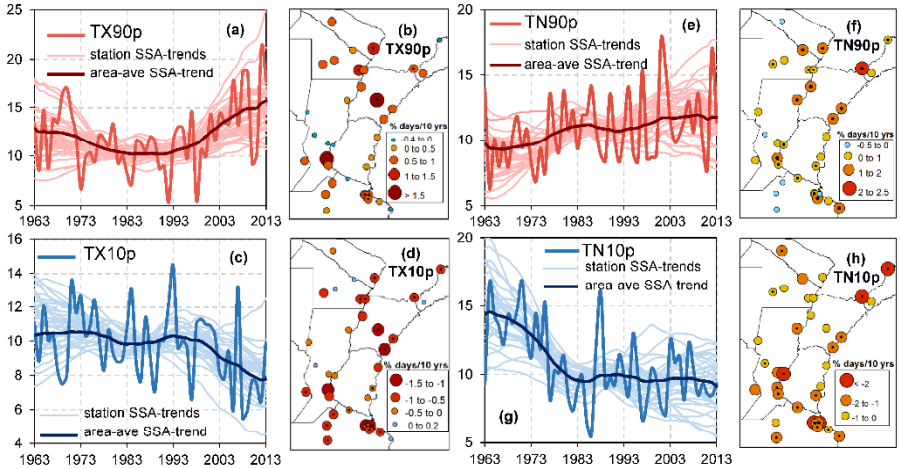

Fig. 2: Frequency of maximum and minimum temperature climate extremes characterized by warm and colds days (TX90p and TX10p) and warm and cold nights (TN90p and TN10p) respectively. The temporal evolution of the area-averaged indices and their trends (panels a, c, e, g). The spatial distribution of the linear trends (black dots indicate a significant linear trend, at least at the 95% confidence level; panels b, d, f, h). Adapted from Lovino et al. (2018).

3.2. Precipitation-related climate extremes

We characterize the intensity of precipitation-related climate using the annual maximum 1-day precipitation (RX1day) and the simple daily intensity index (SDII) (see Table 1). The area-averaged evolution of RX1day in Fig. 3a indicates that maximum 1-day precipitation events have increased from 1970 to about 2000, declining slightly since mid-2000s. The large dispersion in the time series of all stations (thin lines) suggests a large spatiotemporal variability in intense precipitation events. Particularly, NEA exhibits high interannual variability in intense precipitation events as shown by the area-averaged time series of RX1day in Fig. 3a. The more intense events tend to occur during El Niño years (e.g., 1998, 2002). Precipitation events during La Niña years (e.g., 1989, 2008) do not achieve the same intensity. Consistently, we found an ENSO-range periodicity for RX1day (a cycle of 3.6 years accounting for 27% of its variance). Fig. 3b shows that RX1day presents no definite pattern of change, perhaps due to the fact that precipitation is highly variable in NEA.

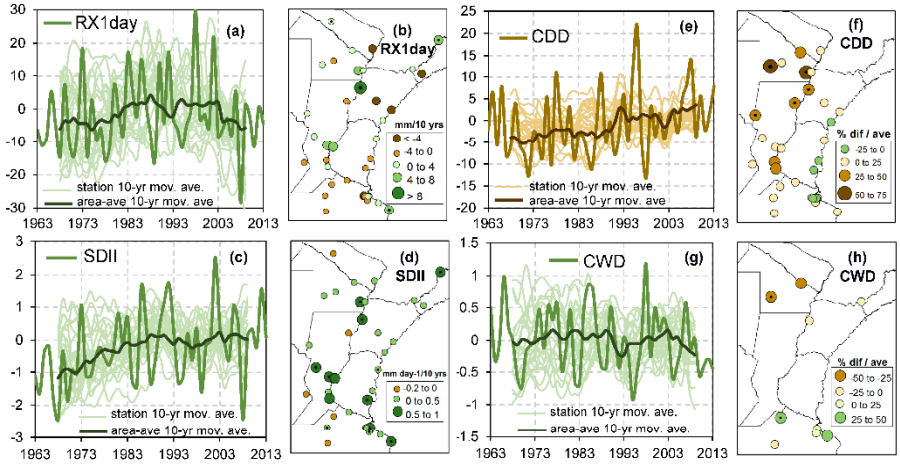

Fig. 3: As in Fig. 2, but for the annual maximum 1-day precipitation amount (RX1day; a-b), the simple daily intensity index (SDII, c-d), the consecutive dry days (CDD; e-f), and the consecutive wet days (CWD, g-h). Linear trends of CDD and CWD are computed in percentage units as the ratio between the linear trend in the 51 years analyzed and the temporal average in the same period for each station. Adapted from Lovino et al. (2018).

The area-averaged 10-yr moving averages series of the SDII (Fig. 3c) shows that precipitation intensity has increased since the early 1970s to the present. Consistently, Fig. 3d indicates that the increase occurred in the whole region, with 31 out of 36 stations showing positive trends (11 of them significant at least at a 95% confidence level). As in the case of RX1day index, the high dispersion in the 10-yr moving averages time series of all stations (Fig. 3c) indicates that the changes in SDII are modulated by large spatiotemporal variability. In particular, SDII is influenced by an interannual variability cycle of 5 years that explains 35% of its variance.

Figures 3e-h present the maximum annual duration of dry and wet spells as characterized by the consecutive dry/wet days indices (CDD and CWD; see Table 1). Fig. 3e shows a continuous increase of dry spell duration since the 1970s (see the time series of the area-averaged 10-yr moving average). Fig. 3f shows a homogeneous pattern of change with 27 stations with positive trends (75% of the total observed stations) increasing the duration of dry spells by 1 to 5 dry days per decade. Notably, the largest increases occurred towards the north, where 5 locations have positive trends that exceed the confidence level of 95%. Figures 3g-h show high interannual variability of wet spell anomalies with no noticeable trend. Fig 3h presents few station with non-significant trends and the rest having no changes (and thus not plotted).

3.3. Temperature- and precipitation-related extremes in reanalyses

So far we have examined extremes as identified by station observations which do not have a complete coverage of the study region. Global reanalysis offer full data

coverage in time and space based on a global model that assimilates diverse kinds of observations. Then, it is of interest to assess whether reanalyses can be used as a complement to observations in northeastern Argentina where there is a limited coverage of gauge stations.

The overall characteristics of the SU25 index are presented in Figs. 4a-c. The spatial field from the reanalysis are superimposed by circles of the corresponding values obtained from observations. A visual inspection suggests that there is similarity between the spatial pattern identified in observations and reanalyses (Figs. 4a-b). NCEP2 overestimates the field of observed summer days towards the south. According to Fig. 6c, the area-averaged SU25 estimated from ERA-Interim follows the temporal evolution of the observations-based SU25 with a mean bias error of only 3 days and a correlation coefficient close to 0.9. However, the interannual variability of the area-averaged SU25 is not properly represented by NCEP2, with a correlation coefficient of 0.51. Pearson correlation coefficients for SU25 index computed from reanalyses at each station location are presented in Fig. 4d-e. ERA-Interim achieves the best performance, particularly towards the south, with most correlations to observations exceeding 0.7. In contrast, the older NCEP2 shows lower values with the most frequent correlations in the range between 0.4 and 0.6.

Figs. 4f-g show that both ERA-Interim and NCEP2 tend to reproduce the spatial mean fields, but underestimate the spatiotemporal variability of frost days, particularly toward the south. The time series of area-averaged frost days (Fig. 4h) exhibit similar variability ($r = 0.86$ for ERA-Interim and $r = 0.87$ for NCEP2) but with a systematic mean bias error of -3 days for NCEP2 and -5 days for ERA-Interim. Fig. 4i-j show that the two reanalyses characterize frost days with similar correlation: the most frequent correlation coefficients range between 0.4 and 0.7.

According to Figs. 4k-l, the observed climatology of RX5day (circles) presents a southwest-northeast gradient that ranges from 125 mm to 200 mm with high spatial variability. Both reanalysis climatologies depict a smoothed version of the observed spatial variability. However, the reanalyses reproduce the temporal variability of the observed RX5day, achieving correlation coefficients close to 0.65. Yet, there are periods (1998-2000) in which large departures are found. Fig 4m shows that ERA-Interim and NCEP2 underestimate the time evolution of area-averaged RX5day by about 16-18 mm, which represents relative errors of about 10-12% with respect to the area-averaged observations. Fig. 4n-o suggest that both reanalyses fail to represent the observed RX5day, as their correlations are lower than 0.2 in the whole region.

4. DISCUSSION AND CONCLUDING REMARKS

The changes in daily temperature extremes reveal a trend towards warmer conditions over northeastern Argentina, which is consistent with what has been observed in other regions of the world (e.g., Donat et al., 2013). Minimum-temperature extremes had a signal of nighttime warming due to a significant increase in warm nights and a significant decrease in cold nights. Maximum-temperature extremes also exhibited a daytime warming resulting from a significant increase in warm days and a

significant decrease in cold days. While the minimum temperature warming seems to have been stabilizing in recent decades, the maximum temperature warming continues to rise.

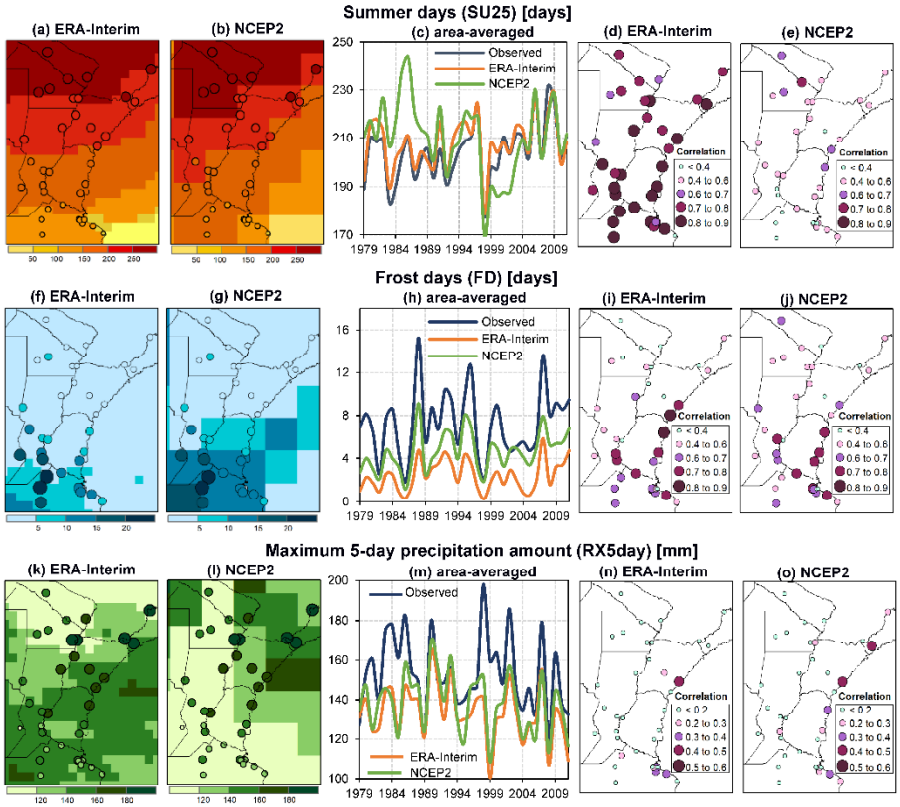

Fig. 4. (a-e) Summer days (SU25), (f-j) frost days (FD), and (k-o) annual maximum 5-day precipitation (RX5day) represented by the ERA-Interim and NCEP2 reanalyses for the period 1979-2011 and compared with observations. Spatial distribution of mean climatology values are given in the first two panels, area-averaged time series of the Argentinian territory in the third panel and correlation coefficient in the last two panels of each row. Adapted from Lovino et al. (2018).

Our results show that intense precipitation events are highly influenced by interannual variability and, although no significant trends were found with the SSA method, a steady increase of mean intensity values occurred since 1970. The annual maximum amount of 1-day precipitation events also increased since 1970, although it seems to be stabilizing in recent years. The observed high variability is influenced by frequent and intense mesoscale convective systems and convective storms (Rasmussen et al., 2016) that cause extreme precipitation events everywhere in the region. The prevalence for few days of convective systems and convective storms also explains the short duration of consecutive wet days. However, during those

days large amounts of precipitation can accumulate leading to severe floods (Cavalcanti et al., 2015). While precipitation has increased, our results show that dry spells in recent decades have tended to last longer, suggesting that more persistent short-term droughts may affect agriculture activities, mainly in the drier area towards the northwest.

Finally, the ERA-Interim and NCEP2 reanalyses have different degrees of success in representing the observed extreme temperature and precipitation events. The ERA-Interim is a newer reanalysis that unlike the older NCEP2 includes assimilation of surface temperature observations. Our findings are in line with this information, as they show that ERA-Interim exhibits greater ability to reproduce the spatial and temporal variability of summer days than NCEP2 over the study region. The two reanalyses represent extreme precipitation events with large biases, which are particularly noticeable when looking at the performance locally at each station. Although both reanalyses tend to recognize the variability of the area-averaged annual 5-day maximum precipitation in time, they underestimate the representation of their spatial distribution. Although reanalyses would be expected to add information for climate extremes in areas of scarce observations like northeastern Argentina, they still need to be used with great caution and as a complement to observations.

ACKNOWLEDGEMENTS

We appreciate the grant from the PRODACT 2018 of the Science and Technical Secretariat (FICH – UNL). This research was carried out with support of Projects CRN3035 and CRN3095 of the Inter-American Institute for Global Change Research (IAI), which is supported by the US National Science Foundation. UNL Project C.A.I. + D. 2016 32/180 is also acknowledged. The NCEP2 climate indices were provided by the Canadian Centre for Climate Modelling and Analysis (Sillman et al., 2013).

REFERENCES

Carril, A. F., Cavalcanti, I. F. A., Menéndez, C. G., Sörensson, A., López-Franca., N., Rivera, J., Robledo, F., Zaninelli, P., Ambrizzi, T., Penalba, O., da Rocha, R., Sánchez, E., Bettolli, M., Pessacg, N., Renom, M., Ruscica, R., Solman, S., Tencer, B., Grimm, A., Rusticucci, M., Cherchi, A., Tedeschi, R., Zamboni, L, 2016. Extreme events in the La Plata basin: a retrospective analysis of what we have learned during CLARIS-LPB project. Clim. Res. 68: 95-116. http://dx.doi.org/10.3354/cr01374.

Cavalcanti, I. F. A., Carril, A. F., Penalba, O. C., Grimm, A. M., Menéndez, C. G., Sanchez, E., Chechi, A., Sörensson, A., Robledo, F., Rivera, J., Pántano, V., Betolli, L. M., Zaninelli, P., Zamboni, L., Tedeschi, R. G., Dominguez, M., Ruscica, R., Flach, R, 2015. Precipitation extremes over La Plata Basin—review and new results from observations and climate simulations. J. Hydrol. 523: 211–230. http://dx.doi.org/10.1016/j.jhydrol.2015.01.028.

Dee, D. P., Uppala, S. M., Simmons, A. J., Berrisford, P., Poli, P., Kobayashi, S., Andrae, U., Balmaseda, M. A., Balsamo, G., Bauer, P., Bechtold, P., Beljaars, A.C.M., van de Berg, L., Bidlot, J., Bormann, N., Delsol, C., Dragani, R., Fuentes, M., Geer, A. J., Haimberger, L., Healy, S. B., Hersbach, H., Hólm, E. V., Isaksen, L., Kållberg, P., Köhler, M., Matricardi, M., Mcnally, A. P., Monge-Sanz, B. M., Morcrette, J.-J., Park, B.-K., Peubey, C., de Rosnay, P., Tavolato, C., Thépaut, J.-N., Vitart, F., 2011. The ERA-Interim reanalysis: configuration and performance of the data assimilation system. Q. J. R. Meteorol. Soc. 137: 553–597. http://dx.doi.org/10.1002/qj.828.

Donat, M. G., Alexander, L., Yang, H., Durre, I., Vose, R., Caesar, J., 2013. Global land-based datasets for monitoring climatic extremes. Bull. Amer. Meteor. Soc., 94, 997–1006. http://dx.doi.org/10.1175/BAMS-D-12-00109.1.

Ghil, M., Allen, M., Dettinger, M. D., Ide, K., Kondrashov, D., Mann, M., Robertson, A., Saunders, A., Tian, Y., Varadi, F., Yiou, P., 2001. Advanced Spectral Method for Climatic Time Series. Rev. of Geop., 40, 1-41. http://dx.doi.org/10.1038/350324a0.

Guha-Sapir, D., Below, R., Hoyois, P., 2015. EM-DAT: International disaster database. Catholic University of Louvain: Brussels, Belgium.

Kanamitsu, M. Ebisuzaki, W., Woollen, J., Yang, S., Hnilo, J.J., Fiorino, M. M., Potter, G. L., 2002. NCEP–DOE AMIP-II Reanalysis (R-2). Bull. Amer. Meteor. Soc., 83, 1631–1643. http://dx.doi.org/10.1175/BAMS-83-11-1631.

Klein Tank, A.M.G., Zwiers, F.W., Zhang, X., 2009. Guidelines on Analysis of Extremes in a Changing Climate in Support of Informed Decisions for Adaptation, WMO-TD No. 1500/WCDMP-No. 72, Geneva. 52 pp.

Lovino, M. A., Müller, O. V., Berbery, E. H, Müller, G. V., 2018. How have daily climate extremes changed in the recent past over northeastern Argentina. Glob. Planet. Chang., 168, 78-97. https://doi.org/10.1016/j.gloplacha.2018.06.008.

Magrin, G. O. Marengo, J. A., Boulanger, J.-P., Buckeridge, M. S., Castellanos, E., Poveda, G., Scarano, F. R., and Vicuña, S., 2014. Central and South America. In: Climate Change 2014: Impacts, Adaptation, and Vulnerability. Part B: Regional Aspects [Barros, V.R., et al (eds.)]. Cambridge University Press, USA, pp. 1499-1566.

Rasmussen, K. L., Chaplin, M.M., Zuluaga, M.D., Houze, R.A., 2016. Contribution of extreme convective storms to rainfall in South America. J. Hydrometeor., 17,353–367. http://dx.doi.org/10.1175/JHM-D-15-0067.1.

Rusticucci, M., Barrucand, M., Collazo, S., 2016. Temperature extremes in the Argentina central region and their monthly relationship with the mean circulation and ENSO phases. Int. J. Climatol., 37: 3003-3017. https://doi.org/10.1002/joc.4895

Sen, P. K., 1968. Estimates of the regression coefficient based on Kendall's tau. J. Am. Stat. Assoc. 63, 1379–1389. https://www.jstor.org/stable/2285891

Sillmann, J., Kharin, V. V., Zhang, X., Zwiers, F. W., Bronaugh, D., 2013. Climate extremes indices in the CMIP5 multimodel ensemble: Part 1. Model

evaluation in the present climate, J. Geophys. Res. Atmos., 118, 1716–1733. http://dx.doi.org/10.1002/jgrd.50203.

Skansi, M. M., Brunet, M., Sigró, J., Aguilar, E., Arevalo Groening, J. A., Betancour, O. J., Castellón Geier, Y. R., Correa Amaya, R. L., Jácome, H., Malherios Ramos, A., Oria, Rojas, C., Pasten, A., Sallons Mitro, S., Villaroel, C., Martínez, R., Alexander, L. V., Jones, P. D., 2013. Warming and wetting signals emerging from analysis of changes in climate extreme indices over South America. Glob. Planet. Chang. 100, 295–307. http://dx.doi.org/10.1016/j.gloplacha.2012.11.004.

Wang, X. L., Swail, V. R, 2001. Changes of extreme wave heights in Northern Hemisphere oceans and related atmospheric circulation regimes. J. Clim., 14, 2204–2220. http://dx.doi.org/10.1175/1520-0442(2001)014<2204:COEWHI>2.0.CO;2.

Young, K. C., 1992. A three-way model for interpolating monthly precipitation values. Mon. Wea. Rev., 120, 2561–2569. http://dx.doi.org/10.1175/1520-0493(1992)120<2561:ATWMFI>2.0.CO;2.